

# EVALUATION OF THE ROLE OF DIFFUSE SCATTERING IN URBAN MICROCELLULAR PROPAGATION

Vittorio Degli-Esposti\*, Henry L. Bertoni\*\*

\*Università di Bologna - Dipartimento di Elettronica, Informatica e Sistemistica  
Villa Griffone Radio Lab - 40044 Pontecchio Marconi - Bologna - Italy  
e-mail: vdegliespsti@deis.unibo.it

\*\*Polytechnic University - Department of Electrical Engineering  
Six Metrotech Center, Brooklyn, NY, 11201 USA  
e-mail: hbertoni@poly.edu

## ABSTRACT

The role and the importance of diffuse scattering in urban radio propagation is evaluated using a new, simple analytical scattering model and a ray tracing tool.

The scattering model is arranged so that the main parameters, having a precise physical meaning, can be easily tuned using classical measurement or simulation results reported in the literature. A basic urban topology has been considered and the impact of diffuse scattering on narrowband as well as wideband propagation parameters has been investigated. Although the scattering parameters have been underestimated (with respect to literature data) in order for the evaluation to be more conservative, the scattering contribution has shown to be very important for both received power and channel dispersion in a variety of cases.

## I - INTRODUCTION

Third generation wireless personal communication services, with their high-speed, multimedia transmission will require a deep and complete understanding of the RF propagation channel in order to be properly designed, deployed and optimized.

In this framework, reliable and fast wideband field prediction tools will become fundamental.

Recently, the development of Ray Tracing (RT) tools has greatly improved microcellular field prediction capabilities and remarkable results have been obtained in a variety of cases [1-7]. However, since RT only accounts for rays that undergo specular reflections or diffractions, it still fails to properly describe diffuse scattering phenomena which can have a significant impact on propagation. According to preliminary studies and to some literature results [8, 9], RT sensibly underestimates channel dispersion in some typical urban microcellular topologies such as rectilinear street canyons and T-shaped or X-shaped street intersections. Similar problems occur for angle of arrival or fading statistics or even field strength in particular, obstructed LOS (Line Of Sight) cases. With the arrival of future

wideband, millimeter wave wireless services, diffuse scattering will probably become even more important due to the higher frequency.

Besides some promising preliminary assessments, little has been done so far to model diffuse scattering in urban environment in an efficient way. Diffuse scattering has often been studied as a phenomenon perturbing specular reflection on rough surfaces [10] or attenuating propagation through vegetation [11]. Only few publications deal with the evaluation of diffuse scattering itself for microcellular field prediction purposes [12-15].

As used here, diffuse scattering refers to the signals scattered in other than the specular direction as a result of deviations in a building wall from a smooth flat layer. Windows, balconies, irregular brick or stone work, internal beams, and differences in materials are examples of the sources of diffuse scattering. These sources can be thought of as an *effective roughness* associated with each building wall. The adopted scattering model is suited for efficient, wideband urban propagation field prediction. The scattering contribution of each wall is computed directly from distances and orientations with respect to Tx and Rx using a simple, analytic formula that depends on few scattering parameters (see section II). These parameters, having a precise physical meaning, can be easily tuned using measurement or simulation results reported in the literature. The scattering model has been integrated into a RT-UTD (Uniform Theory of Diffraction) prediction tool. The final purpose of the work is to evaluate the significance of diffuse scattering in urban microcellular propagation by comparing the effect of the scattered fields to that of reflected/diffracted fields on field strength or RMS delay spread for wideband sources.

In order for the evaluation to be more conservative, the scattering parameters have been underestimated with respect to literature data. Nevertheless, results show that diffuse scattering can sensibly affect both received power and channel dispersion in typical urban topologies.

## II - THE DIFFUSE SCATTERING MODEL

As stated in the introduction, diffuse scattering is assumed to spring from wall surfaces. Each wall is associated a scattering coefficient  $S$  and a reflection loss factor  $R$ . The scattering coefficient  $S$  is defined as the ratio between the local scattered field and the incident field. The loss factor  $R$  accounts for the loss of power in the specularly reflected wave and is a well known parameter of scattering theory [16].

Let  $dS$  be an infinitesimal surface element belonging to a building wall (see Fig. 1). A Lambertian scattering pattern for each surface element is assumed, that is, the scattered wave is a non-uniform spherical wave whose amplitude  $E_s$  is expressed by  $E_s = E_{so} \sqrt{\cos(\theta_s)}$ . Let's now consider a ray tube of solid angle  $d\Omega$  impinging on the surface element. Part of the power is reflected toward the destination point  $D$  in the specular ray tube, also of solid angle  $d\Omega$ , part is transmitted and part is scattered in the upper half space.

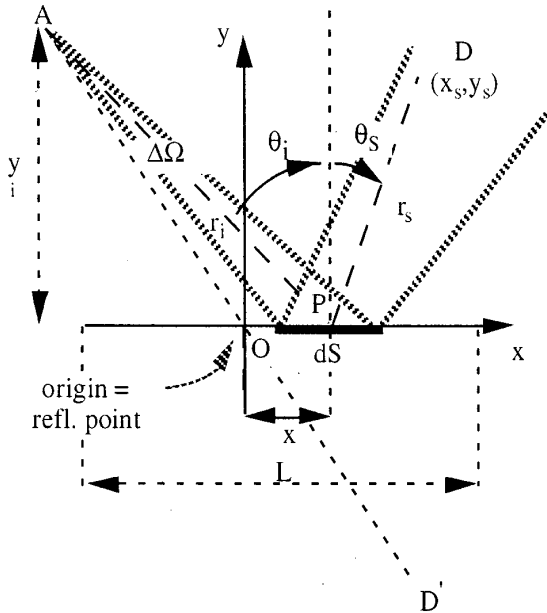


Figure 1 - 2D view in the  $xy$  plane with the surface element  $dS$  located at a distance  $x$  from the reflection point

Since the solid angle of the scattered "tube" is  $2\pi$  a new distance-decay law must be applied. By expressing the power flowing through the tubes as the product of the power densities and the cross section of the tubes the following relations can be found:

$$1) |\Gamma|^2 E_i^2 \Delta\Omega r_i^2 = E_r^2 \Delta\Omega (r_i + r_s)^2$$

(reflected field)

$$2) \quad S^2 E_i^2 \Delta\Omega r_i^2 = \int_0^{\frac{\pi}{2}} \int_0^{2\pi} E_s^2 r_s^2 \sin\theta_s d\theta_s d\varphi$$

$$= \int_0^{\frac{\pi}{2}} \int_0^{2\pi} E_{so}^2 \cos\theta_s r_s^2 \sin\theta_s d\theta_s d\varphi = E_{so}^2 \pi r_s^2$$

(scattered field)

where  $E_i$ ,  $E_s$  and  $E_r$  are the incident, scattered and reflected field amplitudes, respectively, and  $\Gamma$  is the reflection coefficient. From 2) one can obtain

$$3) \quad E_s = S \sqrt{\frac{\Delta\Omega \cos\theta_s}{\pi}} \frac{r_i}{r_s} E_i$$

Since  $E_i$  is proportional to  $(1/r_i)$  and  $\Delta\Omega = (dS \cos\theta_i / r_i^2)$ , from 3) we have:

$$4) \quad E_s = K_0 S \sqrt{\frac{dS \cos\theta_i \cos\theta_s}{\pi}} \frac{1}{r_i r_s}$$

where  $K_0$  is a constant depending on the amplitude of the impinging wave.

Since the power scattered by the single surface element comes at the expense of the reflected power or from the power penetrating the surface of the wall ( $P_p$ ), the following power budget holds:

$$E_i^2 \Delta\Omega r_i^2 = |\Gamma|^2 R^2 E_i^2 \Delta\Omega r_i^2 + S^2 E_i^2 \Delta\Omega r_i^2 + 2\eta P_p$$

where  $\eta = 377\Omega$  is the intrinsic impedance of vacuum. Therefore we obtain:

$$5) \quad 1 = |\Gamma|^2 R^2 + S^2 + \frac{P_p}{P_i}$$

where  $P_i$  is the incident power. If we assume that  $P_p/P_i$  depend only on the average electromagnetic characteristics of the wall, then the power scattered by equivalent surface roughness reduces the reflected power; that is, the greater  $S$ , the lower  $R$ .

It is possible to obtain a rule-of-thumb evaluation of  $R$  and  $S$  as follows.  $R$  may be determined by applying the theory of scattering from rough surfaces as a function of the standard deviation of surface roughness [16]. Alternatively  $S$  could be determined from scattered field

measurements. In [10] measurements are reported for a limestone wall. At normal incidence the estimated magnitude of the reflection coefficients is of about 0.5 if the surface is smooth, and 0.3 if the surface is rough with a standard deviation  $\sigma_h=2.5$  cm. According to 5) this corresponds to  $R=0.6$  and  $S=0.4$ . Since usual building walls are far more irregular than a limestone wall, we deem that  $S=0.4$  is a reasonable choice to perform realistic and conservative assessments. In the present work we set  $S=0.316$ : according to the definition of  $S$  this corresponds to assuming that 10% ( $S^2=0.1$ ) of the impinging power is scattered by the wall. Moreover the reflected/diffracted contribution is overestimated by setting  $R=1$ .

### III - IMPULSE RESPONSE FOR A CANONICAL SURFACE

An analytical expression for the impulse response is presented here for an idealized building geometry. These results provide a computational unit in the RT tool that is subsequently used to find the impulse response in realistic building environments. The idealized geometry consists of a Tx and Rx located in front of a flat wall of height  $H$ , as shown in top view in Figure 1. Here  $x$  is the coordinate along the wall, and its origin is taken to be the specular reflection point. The Tx is located at a distance  $y_i$  in front of the wall and Rx is at a distance  $y_s$ . The height  $H$  of the wall is assumed to be small enough compared to the horizontal dimensions so that we can neglect the difference in delay of the fields scattered at different heights in a vertical strip of the wall. With this assumption  $H$  appears simply as a multiplying constant in the scattered power.

Let  $t$  be the time delay of the fields scattered from a vertical strip of the wall located at  $x$ . The dependence of  $t$  on  $x$  can be inverted to give

$$6) \quad x(t) = \frac{a \pm \sqrt{a^2 + bd}}{b},$$

where:

$$\begin{aligned} a &= [2x_s(1+\gamma)] [y_i^2 - y_s^2 - (tc)^2 - x_s^2(1-\gamma^2)] + \\ &+ 4(tc)^2 x_s \\ b &= 4(tc)^2 - [2x_s(1+\gamma)]^2 \\ d &= [y_i^2 - y_s^2 - (tc)^2 - x_s^2(1-\gamma^2)]^2 + \\ &- 4(tc)^2 x_s^2 - 4(tc)^2 y_s^2 \end{aligned}$$

and  $c$  is light speed. The sign "-" or "+" in 6) must be used when  $x>0$  or  $x<0$ , respectively, that is, the  $x$ -domain must be split in two and the

corresponding contribution separately computed and summed at the end.

By substituting (6) into (4), it is found that

$$7) \quad E_s^2 = K_o^2 S^2 \frac{H}{\pi} \frac{x'(t)}{\frac{y_i y_s}{\left[ (x(t) + x_s \gamma)^2 + y_i^2 \right]^{\frac{3}{2}} \left[ (x_s - x(t))^2 + y_s^2 \right]^{\frac{3}{2}}}},$$

where  $y_i$  and  $y_s$  are the distances of A and D from the wall, respectively,  $x_s$  is the distance along  $x$  from D to the reflection point ( $x=0$ ) and  $\gamma=y_i/y_s$  (see figure 1). Equation (7) gives a simple, fast, analytical formulation of the scattered field contribution to the power delay profile and can be easily integrated into a microcellular field prediction tool.

### IV - RESULTS

The models described in section II and III have been integrated into a RT-UTD prediction tool [4] and simulations have been performed to compare the magnitude of scattering contribution with the magnitude of reflection/diffraction contribution (RT-contribution in the following) to the total field. A typical, X-shaped street intersection has been considered. When computing  $\Gamma$  from the Fresnel formulas, the relative permittivity and the conductivity of building walls have been set to 5 and  $0.01 [\Omega^{-1} \text{ m}^{-1}]$ , respectively. All rays undergoing up to 5 multiple reflections/diffractions have been computed with the RT-UTD tool. All diffuse scattering contributions due to walls visible from both Tx and Rx have been computed using equations (4) and (7). For wideband assessments, impulses responses have been filtered by performing a convolution with a Gaussian pulse with standard deviation  $\sigma=2\text{ns}$  in order to bypass singularities (Dirac pulses) while preserving the original power of each pulse. Tx and Rx have been placed at a distance of 30 to 190 m from the center of the street intersection with a step of 20m. All  $9 \times 9 = 81$  distance combinations have been simulated. Radio terminals have been equipped with half-wavelength dipoles and the emitted power is 1W.

In Figure 2 the ratio  $R_p = P_s/P_r \cdot 100$  is plotted for all 81 Tx/Rx distances ( $D_T$  and  $D_R$ ), where  $P_s$  is the scattering contribution and  $P_r$  is the RT-contribution to received power. It is interesting to note that scattering is very important in a hyperbola-shaped region, where  $P_s$  is comparable to,  $P_r$ . Figure 3 shows the scattered and RT impulse response for  $D_T=30$ ,  $D_R=190$ : in this case scattering pulses (dotted line) overshadow the RT contribution (solid line).

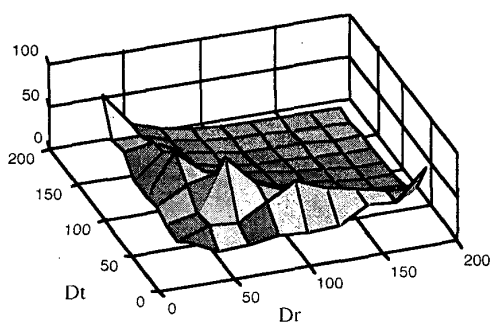


Figure 2 -  $R_p = P_s/P_r * 100$  plotted against Tx and Rx distances from the center of the street intersection ( $D_t$  and  $D_r$ , respectively).

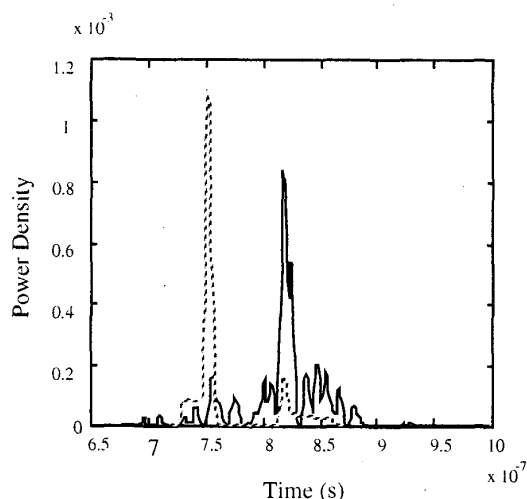


Figure 3 - Scattered (dotted line) and RT-computed (solid line) impulse response for  $D_t = 30$  and  $D_r = 190$ .

In Figure 4 the delay spread (DS) vs.  $D_r$  is reported for  $D_t$  equal to 30, 90, and 170m considering only the RT-contribution. The corresponding results considering both the RT and the scattering contributions is shown in Figure 5. It is evident that diffuse scattering has a great impact on both the absolute DS value and on its dependence on  $D_t$  and  $D_r$ .

## V - CONCLUSIONS

The relevance of diffuse scattering as a major propagation mechanism in urban microcellular environment has been investigated in the paper. An analytical scattering model is presented that is

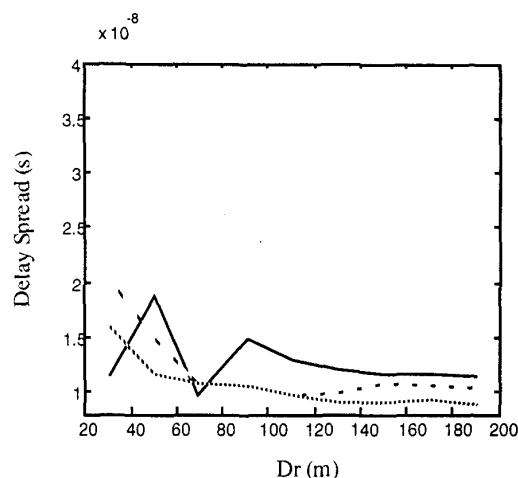


Figure 4 - Delay spread vs.  $D_r$  for  $D_t$  equal to 50m (solid line), 90m (dashed line), and 170m (dotted line) considering only the RT-contribution.

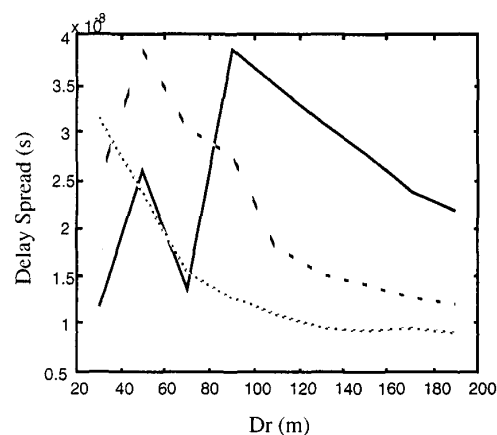


Figure 5 - Delay spread vs.  $D_r$  for  $D_t$  equal to 50m (solid line), 90m (dashed line), and 170m (dotted line) considering both the RT and the scattering contributions

suit for efficient, wideband microcellular field prediction. The scattering model has been integrated into a RT-UTD prediction tool in order to compare the scattering contribution with the reflection/diffraction contribution to the total field in terms of field intensity and delay spread.

Although the scattering parameters have been conservatively estimated with respect to literature data, nevertheless, the results show that diffuse scattering can sensibly affect both received power and channel dispersion in typical urban topologies. In particular, diffuse scattering seems to play a key role in the street corner effect, contributing to received power beyond the line of

sight boundary and determining a sensible delay spread increase.

## VI - ACKNOWLEDGEMENTS

The authors would like to thank the Italian National Research Council (CNR) for having partially funded this research.

## REFERENCES

- [1] H. R. Anderson, "A Ray-Tracing Propagation Model for Digital Broadcast Systems in Urban Areas" *IEEE Trans. Broad.*, vol. 39, pp. 309-317, September 1993.
- [2] T. Kürner, D. J. Cichon and W. Wiesbeck, "Concepts and results for 3D digital terrain-based wave propagation models: an overview," *IEEE Journal on Selected Areas in Communications*, Vol. 11, No. 7, pp.1002-1012, September 1993.
- [3] H. L. Bertoni, W. Honcharenko, L. R. Maciel and H. H. Xia, "UHF propagation prediction for wireless personal communications," *IEEE Proceedings*, vol. 82, no. 9, pp.1333-1359, Sept. 1994.
- [4] Pietro Daniele, Vittorio Degli-Esposti, Gabriele Falciasecca, Guido Riva, "Field prediction tools for wireless communications in outdoor and indoor environments", *IEEE MTT-S European Topical Congress "Technologies for Wireless Applications"*, Turin, Italy, pp. 129-134, November 2-4, 1994.
- [5] M. C. Lawton and J. P. McGeehan, "The application of a deterministic ray launching algorithm for the prediction of radio channel characteristics in small-cell environments," *IEEE Trans. Veh. Technol.*, vol. 43, pp.955-969, Nov. 1994.
- [6] S. Y. Tan and H. S. Tan, "Propagation model for microcellular communications applied to path loss measurements in Ottawa city streets," *IEEE Trans. Veh. Technol.*, vol. 44, no. 2, pp.313-317, May 1995.
- [7] G. Liang and H. L. Bertoni, "A new approach to 3D ray tracing for propagation prediction in cities," *IEEE Trans. Ant. Propagat.*, vol. 46, no. 6, pp.853-863, June 1998.
- [8] T. Takeuchi, M. Sako and S. Yoshida, "Multipath delay prediction on workstation for urban mobile radio environment," *Electronics Letters*, vol. 28, no. 15, pp.1381-1382, 16th July 1992.
- [9] U. Kauschke, "Propagation and system performance simulation for the short range DECT system in microcellular urban roads," *IEEE Trans. Veh. Technol.*, vol. 44, no. 2, pp.253-260, May 1995.
- [10] O. Landron, M. J. Feuerstein and T. S. Rappaport, "A comparison of theoretical and empirical reflection coefficients for typical exterior wall surfaces in a mobile radio environment," *IEEE Trans. Ant. Propagat.*, vol. 44, no. 3, pp.341-351, March 1996.
- [11] S. A. Torrico, H. L. Bertoni and R. H. Lang, "Theoretical investigation of foliage effects on path loss for residential environments," *46th Vehicular Technology Conference*, pp.854-858, Atlanta, April 28-May 1, 1996.
- [12] K. R. Shaubach, N. J. Davis, and T. S. Rappaport, "A ray tracing method for predicting path loss and delay spread in microcellular environments," *42th Vehicular Technology Conference*, pp.932-935, Denver, May 1992.
- [13] M. O. Al-Nuaimi and M. S. Ding, "Prediction models and measurements of microwave signals scattered from buildings," *IEEE Trans. Ant. Propagat.*, vol. 42, no. 8, pp.1126-1137, August 1994.
- [14] H. R. Anderson, "A second generation 3-D ray-tracing model using rough surface scattering," *46th Vehicular Technology Conference*, pp.46-50, Atlanta, April 28-May 1, 1996.
- [15] C. Kloch, J. Bach Andersen, "Radiosity - an approach to determine the effect of rough surface scattering in mobile scenarios", *IEEE AP-S International Symposium*, pp 890-893, Montreal, July 1997.
- [16] W. S. Ament, "Toward a theory of reflection by a rough surface," *Proc. IRE*, vol. 41, n. 1, pp.142-146, Jan 1953.